Hindawi
Shock and Vibration
Volume 2018, Article ID 1623103, 18 pages
https://doi.org/10.1155/2018/1623103

Research Article

Mechanical Performance and Design Method of Improved Lead Shear Damper with Long Stroke

Baoshun Wang, Weiming Yan, and Haoxiang He

Beijing Key Laboratory of Earthquake Engineering and Structural Retrofit, Beijing University of Technology, Beijing 100124, China

Correspondence should be addressed to Haoxiang He; hhx7856@163.com

Received 2 July 2017; Revised 12 November 2017; Accepted 2 January 2018; Published 29 January 2018

Academic Editor: Felice Ponzo

The paper presents experimental study on an improved plate lead shear damper with long stroke (ILSD-LS) which is developed to meet the engineering requirements for high-rise structures with long periods subjected to the long-period earthquakes. Finite element analysis is also carried out to investigate the proposed damper. Based on the ideal rigid-plastic constitutive law of lead, a mechanical model of the ILSD-LS is established. Compared with ordinary dampers, ILSD-LS has better damping force, energy dissipation capacity, and stability according to the results of simulation and experiments. The method of calculating damping force is reasonable and accurate. In order to verify the damping effect of ILSD-LS for the structures with long periods under long-period ground motions, the nonlinear time history analysis of a typical high-rise structure with ILSD-LS is carried out. The numerical results indicate that the seismic responses of the high-rise structure with ILSD-LS are significantly reduced when subjected to long-period ground motion.

1. Introduction

Earthquake can generate huge loss and damage to human beings and society, so it is meaningful to study the dynamic effect of ground motion on structure and to reduce structural vibration with high-performance dampers.

According to epicentral distance, ground motion can be divided into the near-field earthquake and the far-field earthquake, and the far-field vibration is also called long-period ground motion. In earthquake engineering, long-period ground motion usually refers to the ground motion whose predominant period ranges from 2 s to 10 s, and long-period components are abundant in this range [1]. Long-period ground motion is often characterized by relatively low acceleration, low frequency components mainly concentrated in the later stage, large velocity and displacement, long duration, and so on. The previous earthquake damage phenomena show that the tall building structures with long periods may generate large horizontal displacement and serious damage under the action of far-field earthquake with rich long-period components. In addition, with the development of city construction and the increasing social demand, the form of high-rise building structure is becoming more flexible and complex. For typical high-rise buildings such as large span structure, tall structure, and long-span suspension structure, they have longer natural periods and many of them are important lifeline projects; the seismic performance is very important for the normal use of structures and the safety of public life. Hence, it is necessary to carry out seismic research and structural control technology of long-period structures.

In civil engineering structure, the structural control technology is developing vigorously. The control system mainly reduces the structural vibration to prevent damage to structures subjected to natural disasters such as wind and earthquake. The structure can be controlled by the active control system and the passive control system. Since the active control system needs to input higher external energy and has higher developing costs, the passive control system is preferred in general structures. Passive control system mainly uses energy dissipation components such as dampers to dissipate dynamic energy. The main dampers currently include friction dampers, viscoelastic dampers, viscous dampers, metal dampers, and tuned mass dampers, and the corresponding theoretical research and technology

are intensively studied. If the traditional dampers are installed on the high-rise building structure, the structural deformation maybe exceeds the effective stroke of the damper under long-period ground motion, so the performance of the damper is not fully exploited; even the damper itself could fail. Therefore, it is necessary to use large stroke dampers to reduce vibration for high-rise building structure subjected to long-period earthquake. Compared with the traditional damper, the requirements of the composition, design scheme, and production accuracy for the large stroke damper are higher; the stroke especially should fully meet the engineering demand, and the stroke distance is usually in tens of centimeters. At present, the research on the structure and mechanical properties and design method of large stroke damper has a promising tendency towards development, so it is necessary to carry out in-depth theoretical and experimental research.

In order to develop long-stroke dampers, the characteristics and the potential of various traditional dampers can be considered. Friction damper has the strong capacity of energy dissipation; the load frequency has little influence on the performance, and it has the advantages such as simple structure, easy material selection, and low cost. However, the friction damper's performance relies on the materials' long-term static contact in the constant positive pressure, which will produce cold bonding or solidification. The desired coefficient of friction cannot be guaranteed, and loading cycles will also dramatically reduce the friction coefficient of the damper; this makes the friction device unfavorable. In addition, the friction damper will produce permanent deviation after large displacement of structure occurs. It also needs maintenance and protection, so its energy dissipation capacity is limited [2–4].

Viscoelastic dampers can dissipate energy with small vibration amplitudes, and they have stable dynamic performance and strong capacity of energy dissipation under different loading frequencies and cycle numbers. However, its energy dissipation capacity decreases with the increase of temperature and strain amplitude [5–7]. Although viscous damper has strong capacity of energy dissipation under small deformation, it has low efficiency of shock absorption and no additional stiffness to the main structure. Therefore it is hard to meet the performance requirements for strong earthquake or large deformation [8–10].

As a typical kind of metal damper, low-yield point steel damper has the advantages of stable hysteretic characteristics, simple structure, and easy replacement after the earthquake, and so on. However, it will cause distortion of hysteresis loop if the shape of low-yield point damper is not suitable. In addition, the damper can just play a role in the strong earthquake, and it accumulates deformation in the earthquake and wind excitation; the hardening of steel makes the seismic response of the structure seriously inconsistent with the design [11–14].

Although the tuned mass damper (TMD) is easy to install, maintain, and replace, the TMD has a damping effect on the structure only for limited tuning frequency bands, and severe time-delay phenomenon may occur especially when large structural deformations appear [15–18]. Therefore, it will inevitably cause defects and hidden dangers to directly enlarge the stroke of these dampers or simply adjust them into large stroke dampers.

Compared with other metal materials, lead has advantages of high density, high stiffness, good flexibility, and ductility, and a large amount of energy can be absorbed during its deformation. Since the melting point of lead is lower, deformation will take place during dynamic recovery and dynamic recrystallization process. In theory, the cumulative fatigue phenomenon will not occur after the plastic cyclic at room temperature. Therefore, the lead damper has the advantages of high energy dissipation and stable performance and it is suitable for the engineering requirement of long-stroke dampers. At present, the typical lead dampers in civil engineering application include lead extrusion damper [19, 20], lead shear damper [21, 22], and cylindrical damper [23]. Lead shear damper has been extensively used in practical engineering. Robinson and Greenbank firstly proposed one such device that was an energy absorber extruding lead back and forth through an orifice [24]. Tsai et al. have tested and explored the characteristics of the new lead extrusion damper (LED). The test results showed that the new LED possessed excellent capability for energy absorption. The hysteresis loop behaved like "plastic solids" or "coulomb dampers." The internal force and the speed of the movement were correlated while the damper was subjected to harmonic loadings. By comparing the numerical results obtained from the proposed analytical model with experimental results under various displacements and frequencies, Tsai et al. concluded that a good agreement between the computational and experimental results has been achieved [20]. Curadelli and Riera proposed a new type of lead ring shearing metal damper of energy dissipation and established relevant design and performance measurement methods [22]. Monti and Robinson proposed a damper based on shear deformation of lead, and the effectiveness of the device was proved by experimental research and theoretical analysis. The damper could be used in buildings or industrial structures to resist external excitations such as wind, earthquake, and traffic [25].

Although the research on the seismic performance of the traditional lead damper is sufficient, there is still a lack of study on the effect of lead damper on high-rise structures subjected to long-period ground motion. The research on the structure and seismic performance with long-stroke lead shear damper is also relatively limited.

Ni et al. designed a magnetorheological damper with large stroke, in which the damping effect was studied through a scaled adjacent structural system consisting of a 12-story building model and an 8-story building model, and a shaking table test was carried out. The results showed that the magnetorheological (MR) damper of large stroke provided effective damping effect, but the location of the damper was the main factor affecting the control efficiency [26]. Behrens et al. proposed an electromagnetic shunt damper (EMSD). It required small shunt voltages, provided large stroke, and reduced the vibration of larger mechanical structures; the theoretical results were also presented [27]. In order to meet the needs of large stroke and large output of high-rise buildings, a new type of intelligent friction damper was proposed based on constrained energy dissipation system by Zhou and Peng

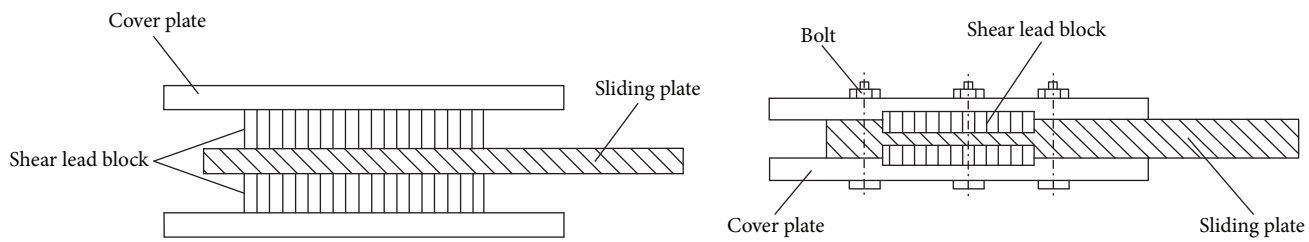

(a) Traditional lead shear damper

(b) Improved lead plate shear damper

Figure 1: Ordinary plate lead shear damper.

[28]. Through the finite element analysis of damper and the nonlinear time history analysis of a structure equipped with dampers, it was proved that the new type of intelligent friction damper had larger friction force and larger allowable displacement, meeting the requirements of engineering applications. Aiming at the demand for viscous dampers with large stroke and strong energy dissipation for the building structures subjected to long time periodic earthquake, Minagawa et al. proposed a viscous-friction hybrid damper as an effective vibration control device suitable for structures having long natural period. The hybrid damper consisted of an oil damper and a friction damper in series [29]. Seismic response analysis of a boiler building with the hybrid damper was carried out, and superior damping performance was confirmed.

Many researchers have also studied the application of long-stroke damper in the seismic design of bridges. Sharabash and Andrawes developed a super elastic shape memory alloy device (SMA). The experiments showed that the stroke of this device could reach 80 mm and the performance of energy dissipation was stable [30]. SMA was applied to the three long-span bridge model; it was shown that the damper could improve the seismic performance of the bridge. Shen et al. proposed a novel system with transverse steel dampers (TSDs) [31]. The experimental results showed that the TSD had excellent performance in energy dissipation, large displacements, and synchronization of triangular plates under complex contact conditions. A 620 m long-span cable-stayed bridge was selected for a case study of the TSD seismic system. The ground motions records considering various site conditions were used as seismic inputs. Numerical results proved that the TSD system had good energy dissipation ability and it was insensitive to the input characteristics of ground motion.

A new type of lead shear damper with capabilities of large deformation was used to achieve energy dissipation by Zhou et al. [21]. It was found that the damping effect of this new damper was as good as normal viscous damper, and leakage and metamorphism did not occur for the new damper. In addition, the new damper was much cheaper than viscous damper. Hence, the lead shear damper has an excellent prospect in structure control. Although the traditional lead plate damper is simpler and cheaper than the magnetorheological damper, friction damper, and viscous damper, it still cannot meet the requirements of large deformation and energy dissipation stability for large structures. Considering theoretical analysis, processing cost, and engineering feasibility, it is significant to develop a new type of lead plate damper with long stroke and high performance.

The previous research provided basic methods and ideas for the design and analysis of lead plate damper with long stroke. However, since the yield point of lead is low and it is hard to fill up during perfusion, the yield force of normal damper is not sufficient, and the capacity of energy dissipation is unstable. Hence, it is necessary to improve the mechanical structure of the current lead plate damper with long stroke to keep its capacity of energy dissipation to be strong and stable during large deformation. Furthermore, the theoretical method of the damper with long stroke should be established. In consideration of the study of long-stroke dampers for building structures not sufficient enough, this study is mainly aimed at investigating the seismic response of long-span or large-deformation building structures with long-stroke dampers.

An improved lead shear damper with long stroke (ILSD-LS) is proposed in this paper; the mechanical model is established, and the finite element simulation is carried out. The actual performance of ILSD-LS is tested by low cycle reciprocating cycle load experiment. The structural time history analysis of high-rise building with ILSD-LS is studied. The results show that the mechanical model of the damper is in good agreement with the experimental results, and the damper has the advantages of large stroke and stable performance.

2. Mechanical Structure of ILSD-LS

The mechanical structure of the traditional lead shear damper is shown in Figure 1(a); the main shortcoming is that the machining requirement of the connection between shear lead block and cover plate is strict; thus the actual yield force of the damper is extremely unstable when longer stroke and larger damping force are needed.

For the improved lead plate shear damper, the mechanical structure is shown in Figure 1(b). Once the stroke exceeds the relative shear length of the lead block, the effective shearing area of lead block rapidly decreases and the output force of the damper declines, so the performance of energy dissipation of the improved lead plate shear damper is still unstable.

To meet the damper requirements of higher yield force and larger stroke for practical engineering, the lead plate

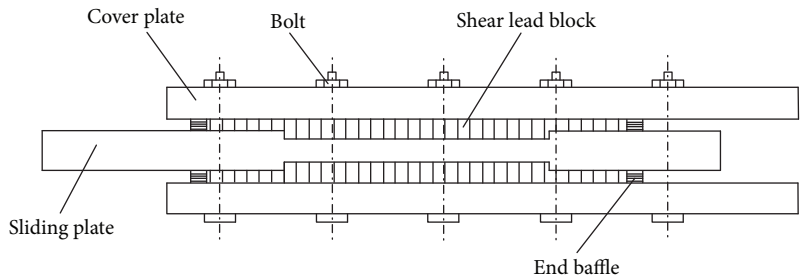

Figure 2: Mechanical structure of LSD-LS.

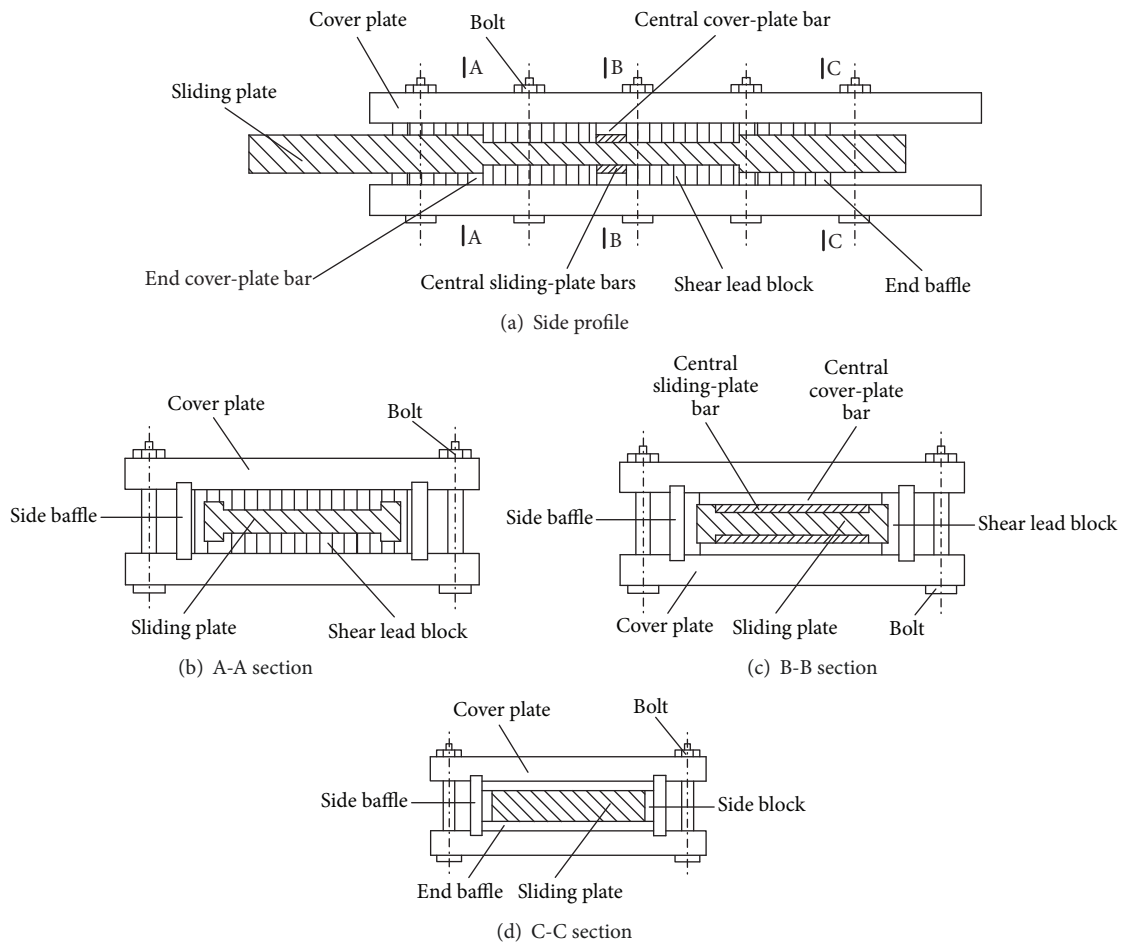

Figure 3: Mechanical structure of ILSD-LS.

shear damper with long stroke (LSD-LS) was proposed by Zhou et al. [21], and the corresponding mechanical structure is shown in Figure 2.

The shear area of lead block in LSD-LS does not decrease during operation but its length in the direction of motion increases, which could allow the lead block to not yield completely in the longitudinal direction. Therefore, the relative shear length of the lead block should be reasonably determined. In addition, LSD-LS cannot meet the requirement of higher yield force for long stroke, and its performance of energy dissipation is still unstable.

In order to overcome the shortages of LSD-LS, an improved lead shear damper with long stroke (ILSD-LS) is proposed in this study, and the corresponding mechanical structure is shown in Figure 3. ILSD-LS is composed of cover plate, sliding plate, side baffle, side block, end baffle, end cover-plate bar, central cover-plate bar, and central sliding plate bar. The two cover plates are placed on the upper and lower positions of the sliding plate, and a groove with the same size is arranged on the upper and the lower surfaces of the slide plate. The side baffle is positioned between the two cover plates, and there is a 10 mm–15 mm distance between

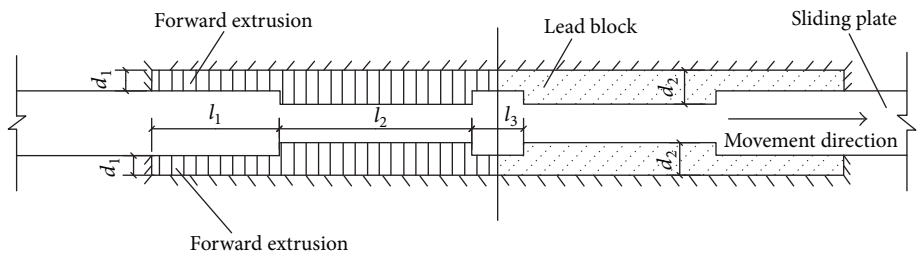

Figure 4: Structure and dimension of ILSD-LS.

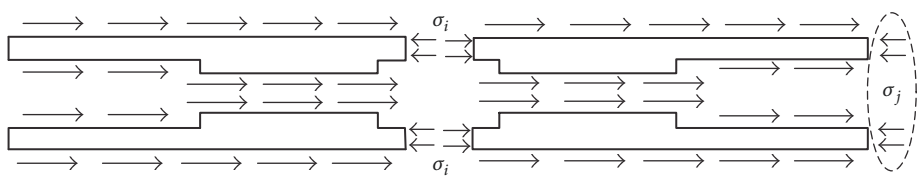

Figure 5: Stress distribution diagram of ILSD-LS.

the side baffle and the slide plate. Two end blocks are welded along the width direction of each cover plate, and there is no gap between the end block and the upper and lower surfaces of the slide plate. Two side blocks are welded in the width direction at the inner end of each side baffle, and there is also no gap between the side block and the slide plate. The inner surfaces of the upper cover plate and the lower cover plate are welded with end cover-plate bar and central cover-plate bar. The central sliding plate bars are respectively welded in the middle part of the two grooves of the sliding plate; besides the end cover-plate bar is required to be separated from the sliding plate without clearance. There is no connection between the central cover-plate bar and the central sliding plate bar, but no clearance exists between both of them. Then a cavity is constituted by fixing cover plate, sliding plate, side baffle, side block, and end baffle by bolts. Finally, the melted lead poured into the cavity solidifies into the block. To reduce the relative shear length of the lead block and ensure the lead block to yield completely, the internal lead block of ILSD-LS is treated separately and the additional constraints are added. The shear lead blocks in the groove will dissipate energy continuously when the sliding plate reciprocally moves.

3. Mechanical Model of ILSD-LS

In traditional analysis, the shear lead block is assumed to generate shear deformation in the axial direction and yield at the same time when the yield force of the shear lead damper is calculated. For ILSD-LS, the lead blocks in the lead grooves are in compressional stress state during the sliding plate reciprocal movements; thus, ILSD-LS can be considered as an extrusion damper. Therefore, the lead in operation can be assumed as ideal rigid plastic material, and the mechanical model of ILSD-LS is established according to the microstress state of lead.

The dimension of the ILSD-LS is shown in Figure 4, and the lateral width of the damper is set as B. Based on the ideal rigid-plastic constitutive law of lead, it is assumed that the shear deformation of the lead is homogeneous and the friction forces of sliding plate, side plate, and lead and side plate are all ignored. In addition, the friction between the lead block and the cover plate is also ignored because the corresponding sliding motion is not significant. Assume the lead block is split along the center line, and stress analysis of the lead block is carried out, as shown in Figure 5. On the basis of the assumption plane-strain, the analytic expression of the normal stress on the center line of the groove is obtained. The specific process is described as follows.

Firstly, the lead blocks in forward compressional stress state are selected as the research object. Since the lead blocks are symmetric and both of lead blocks are spliced in the same direction, their stress diagram is shown in Figure 5. In Figure 6, the lead blocks are divided into six domains according to the flow law of metal in forward compressional stress state, and stress analysis and solution can be carried out for the six domains, respectively.

In Domain I, as shown in Figure 7(a), the antideformation stress of the lead block is assumed as σ_s, which is suggested to be 12.7 MPa [32]. σ_{n1} is the normal stress of lead block interface in Domain I. σ_{n1} approximately equals σ_s. τ_{k1} is the shear stress of lead block interface, μ is friction coefficient, set as 0.15, and τ_{k1} equals $\mu\sigma_s$ according to the friction theorem.

The equation of static equilibrium can be obtained in the horizontal direction, as follows:

$$2\sigma_1 B d_1 = 2\tau_{k1} l_1 B = 2\mu\sigma_s l_1 B. \quad (1)$$

The normal stress on the center line at the end of the Domain I is given by

$$\sigma_1 = \frac{\mu\sigma_s l_1}{d_1}, \quad (2)$$

where d_1 is the thickness of lead block out of groove region and l_1 is the length of lead block in working region.

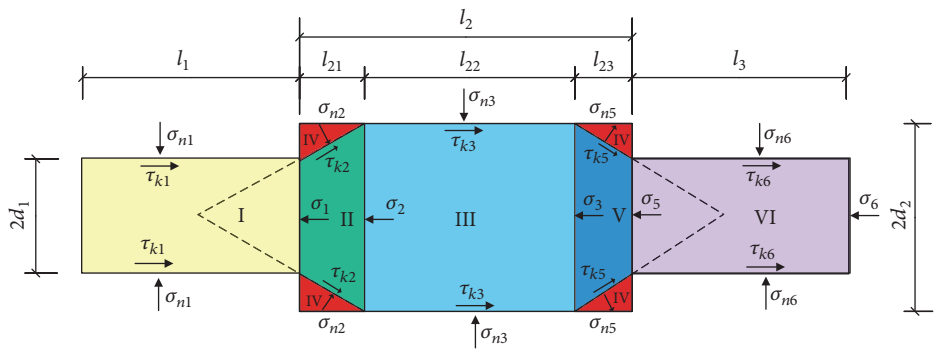

FIGURE 6: Stress diagram of lead in forward compressive state.

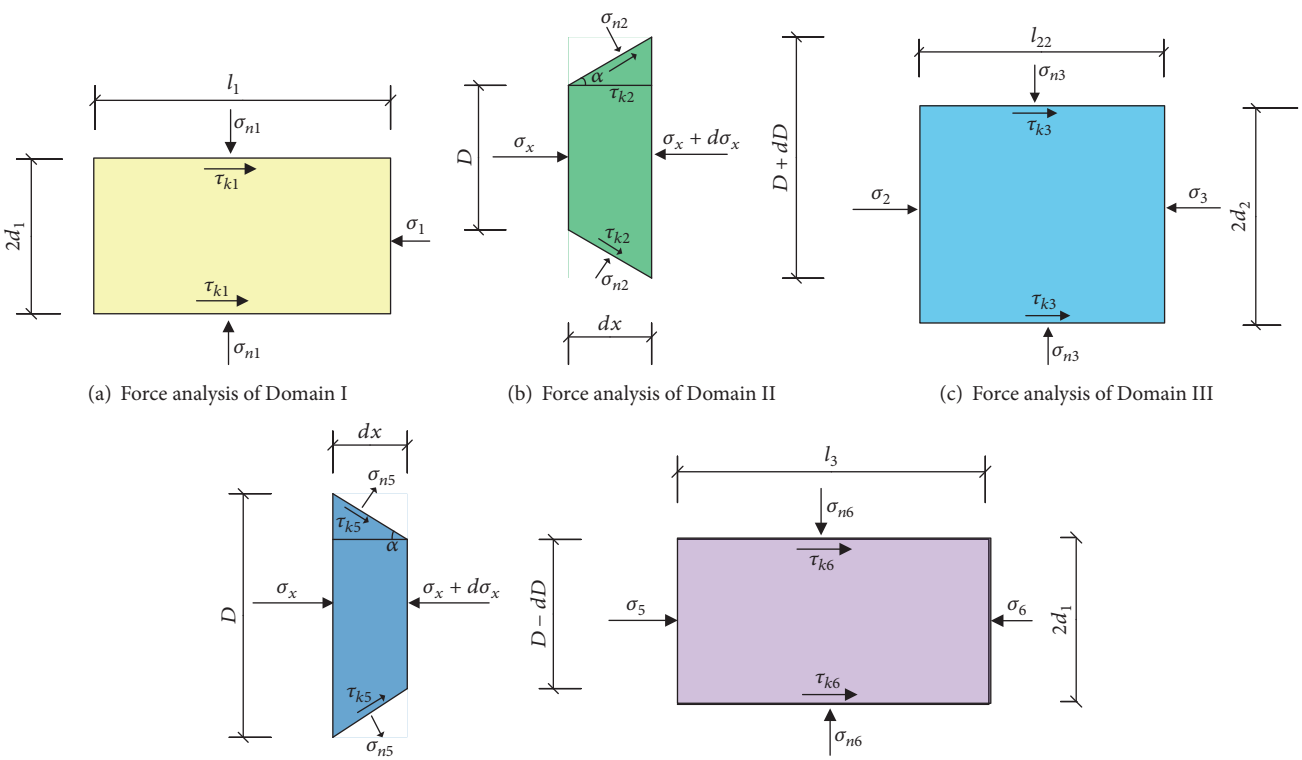

(a) Force analysis of Domain I (b) Force analysis of Domain II (c) Force analysis of Domain III

(d) Force analysis of Domain V (e) Force analysis of Domain VI

FIGURE 7: Stress analysis of lead in the forward compressive state.

The stress state of Domain II is shown in Figure 7(b). As the Domain IV is static during the reciprocating motion of the lead, the shear failure occurs at the cross section of the Domain II and Domain IV, and the corresponding angle of the horizontal plane is α. Thus, the shear stress reaches the maximum $\tau_{\max}$ on the interface between Domain II and Domain IV. If the normal stress of lead block on the interface between Domain II and Domain IV is σ_{n2}, and the corresponding shear stress is τ_{k2}, then $\tau_{k2} = \tau_{\max} = \sigma_s/\sqrt{3}$ can be proved by Von-Mises yield criterion.

The horizontal component of σ_{n2} is

$$T_2 = 2\sigma_{n2} \sin\alpha \cdot \frac{dx}{\cos\alpha} B. \tag{3}$$

The horizontal component of τ_{k2} is

$$T_2' = 2\tau_{k2} B \frac{dx}{\cos\alpha} \cdot \cos\alpha = \frac{2}{\sqrt{3}} \sigma_s B dx. \tag{4}$$

The equation of static equilibrium can be obtained in the horizontal direction of the Domain II as follows:

$$B(\sigma_x + d\sigma_x)(D + dD) - \sigma_x BD - T_2' - T_2 = 0. \tag{5}$$

Consider that the approximate plastic condition $\sigma_{n2} - \sigma_x = \sigma_s$ is acceptable [33], and the geometric relationship $dD = 2\tan\alpha dx$ is obtained, where α is the dead angle and set as 60°. Eq. (5) is integrated with the boundary condition when

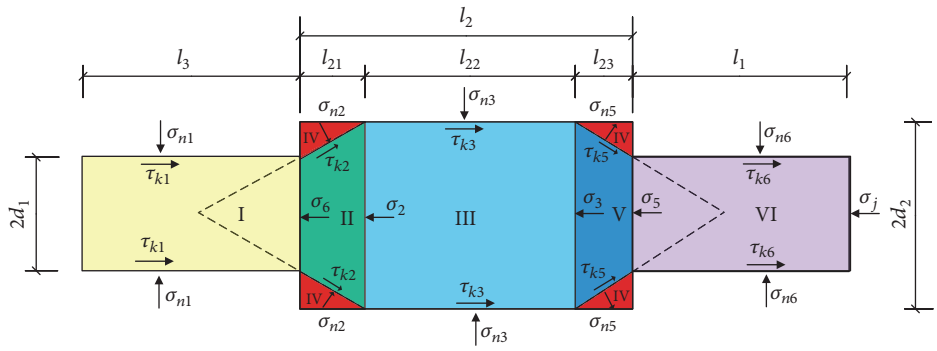

FIGURE 8: Stress diagram of lead in the back forward compressive state.

$D = 2d_1$ and $\sigma_x = \sigma_1$; the normal stress in the center line of Domain II can be obtained

$$\sigma_{2x} = \sigma_s \left[\left(1 + \frac{1}{\sqrt{3}\tan\alpha} \right) \ln \frac{D}{2d_1} + \frac{\mu l_1}{d_1} \right]. \quad (6)$$

If d_2 is the thickness of lead block in groove region and $D = 2d_2$, the normal stress on the center line at the end of Domain II can be obtained by (6), which is expressed as

$$\sigma_2 = \sigma_s \left[\left(1 + \frac{1}{\sqrt{3}\tan\alpha} \right) \ln \frac{d_2}{d_1} + \frac{\mu l_1}{d_1} \right]. \quad (7)$$

In Domain III, as shown in Figure 7(c), the shear stress of the lead block on the upper and lower interfaces is obtained as $\tau_{k3} = \sigma_s/\sqrt{3}$. l_{22} is lead block length in Domain III, and $l_{22} = l_2 - 2(d_2 - d_1)/\tan\alpha$, where l_2 is the length of a single lead groove. The static equilibrium equation in the horizontal direction can be obtained as

$$\sigma_2 \cdot 2d_2 \cdot B + 2\tau_{k3} \cdot l_{22} \cdot B = \sigma_3 \cdot 2d_2 \cdot B. \quad (8)$$

The normal stress on the center line at the end of Domain III can be obtained by (7) and (8) as follows:

$$\sigma_3 = \sigma_s \left[\left(1 + \frac{1}{\sqrt{3}\tan\alpha} \right) \ln \frac{d_2}{d_1} + \frac{\mu l_1}{d_1} + \frac{l_{22}}{\sqrt{3}d_2} \right]. \quad (9)$$

The stress state of Domain V is shown in Figure 7(d); the analysis process is similar to that of Domain II, and the equilibrium equations in the horizontal direction are also established. Finally, the normal stress on the center line at the end of Domain V is obtained as follows:

$$\sigma_5 = \sigma_s \left[2\left(1 + \frac{1}{\sqrt{3}\tan\alpha} \right) \ln \frac{d_2}{d_1} + \frac{\mu l_1}{d_1} + \frac{l_{22}}{\sqrt{3}d_2} \right]. \quad (10)$$

The stress state of Domain VI is shown in Figure 7(e), the analysis process is similar to that of Domain I, and the normal stress on the center line at the end of Domain V is given by

$$\sigma_6 = \sigma_s \left[2\left(1 + \frac{1}{\sqrt{3}\tan\alpha} \right) \ln \frac{d_2}{d_1} + \frac{\mu (l_1 + l_3)}{d_1} + \frac{l_{22}}{\sqrt{3}d_2} \right]. \quad (11)$$

Similarly, according to the above method, if the lead blocks on the other side of the center line of groove are regarded as the research object as shown in Figure 8, the normal stress σ_j, which is on the end of the whole lead block, may be expressed as

$$\sigma_j = \sigma_s \left[5\left(1 + \frac{1}{\sqrt{3}\tan\alpha} \right) \ln \frac{d_2}{d_1} + \frac{\mu (2l_1 + l_3)}{d_1} + \frac{2l_{22}}{\sqrt{3}d_2} \right]. \quad (12)$$

After the normal stress at the end of the whole lead block is obtained by (12), the total yield force P of ILSD-LS is ultimately calculated according to the effective area of the lead block as follows:

$$P = 2\sigma_s \left[5\left(1 + \frac{1}{\sqrt{3}\tan\alpha} \right) \ln \frac{d_2}{d_1} + \frac{\mu (2l_1 + l_3)}{d_1} + \frac{2l_{22}}{\sqrt{3}d_2} \right] Bd_1. \quad (13)$$

For a well-designed lead shear damper, the total yield force is stable and its postyielding stiffness can be ignored due to the small yield displacement, which is usually not greater than 5 mm. Thus, the hysteretic curve of lead damper is generally a standard rectangle, and its mechanical constitutive model is equivalent to an ideal rigid plastic model. Therefore, the mechanical model and the hysteresis curve can be established after the yield force of ILSD-LS is calculated by (13). In the following sections, the correctness and the feasibility of the mechanical model will be verified by numerical simulation and experimental results.

4. Finite Element Simulation and Analysis of ILSD-LS

In order to investigate whether the hysteretic characteristics of ILSD-LS can meet the requirements of large yield force and long stroke for practical engineering, the finite element simulation and analysis of the damper were carried out. The design parameters for ILSD-LS are shown as follows:

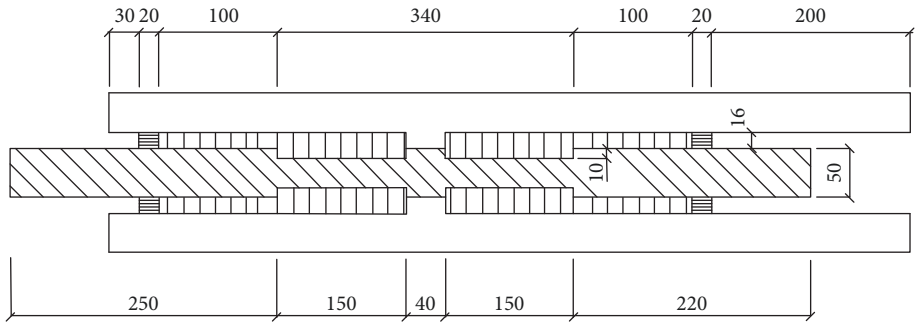

Figure 9: Detail drawing of ILSD-LS (Unit: mm).

B = 200 mm, d_1 = 16 mm, d_2 = 26 mm, l_1 = 100 mm, l_2 = 150 mm, and l_3 = 40 mm. The detailed dimensions are shown in Figure 9. According to the ILSD-LS mechanical analysis model based on (13), the theoretical yield force is 946.1 kN.

Finite element (FE) simulation of ILSD-LS was carried out by ABAQUS software to verify the stability of energy dissipation and the yield degree of the lead blocks in the damper. The FE model is established according to the design dimension, as shown in Figure 10, and the following assumptions are used in the simulation:

(1) According to the construction of ILSD-LS, there is no relative movement between the lead block and the cover plate in horizontal and vertical directions, so the lead block is directly imposed consolidation constraint in the FE mode. The deformation of the sliding plate is ignored because the strength of the sliding plate is much greater than that of the lead block, and it is simplified as a discrete rigid body.

(2) In the initial state, there is no gap or contact between the lead block and the sliding plate, and there is also no interaction between the interfaces. The contact action is simulated by rigid-flexible contact method.

(3) The friction between lead and sliding plate is taken into account, and the friction coefficient is set as 0.7 [34]. The maximum frictional stress on the contact surface is 11.5 MPa.

(4) The material property of lead is assumed to be ideal rigid plastic; although the recrystallization process of lead at room temperature cannot be considered in ABAQUS, it can be equivalent to a stress process by choosing a reasonable strength value of lead. The yield strength σ_y of lead metal is selected as 14.0 MPa, the elastic modulus E is 1.646×10^4 MPa, and Poisson's ratio μ is 0.42 according to the statistical analysis of the experimental data of mechanical properties of lead metal. The yield state of lead material in complex stress state is judged by the Mises criterion.

The FE analysis results of ILSD-LS are illustrated in Figure 11. The yield displacement of the damper is 2 mm, the yield force is 1000.21 kN, and the yield force remains essentially the same with the increase of loading displacement.

When the loading displacement is 90 mm, the stress contour of the whole lead block is shown in Figure 12. The results indicate that the stress of lead block is nearly uniform and the energy dissipation is relatively adequate because the whole section has basically reached the stress yielding state,

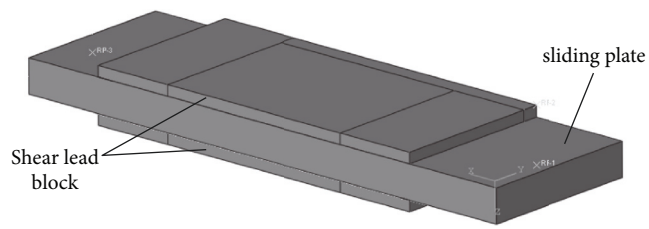

Figure 10: Finite element model of ILSD-LS.

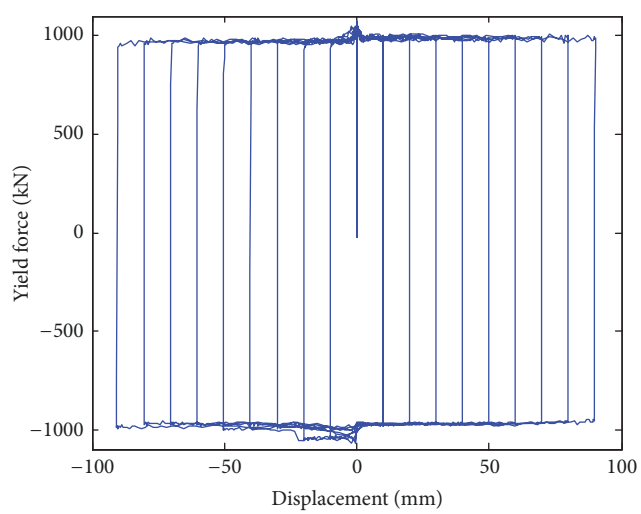

Figure 11: Numerical simulation results of ILSD-LS.

so the ILSD-LS can provide a long stroke with satisfactory stability.

In order to verify the consistency between the theoretical results and the simulation results, the axial normal stress at the end of I–VI domains of the FE model is extracted and compared with the theoretical values, which are shown in Figure 13. It reveals that the theoretical and the simulation results are relatively close. The FE results are larger than the theoretical results mainly due to local stress concentration, which leads to the higher overall average stress of the section. In conclusion, the yield force that is directly based on the

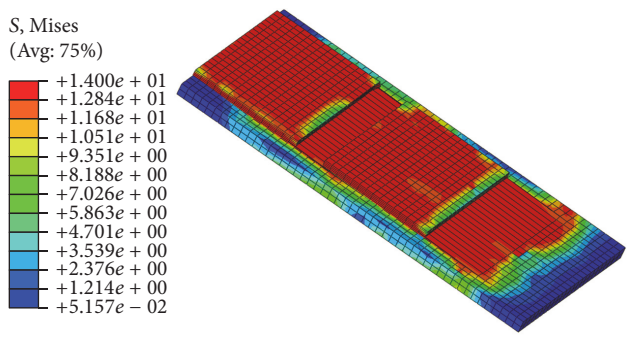

Figure 12: Stress nephogram of displacement 90 mm.

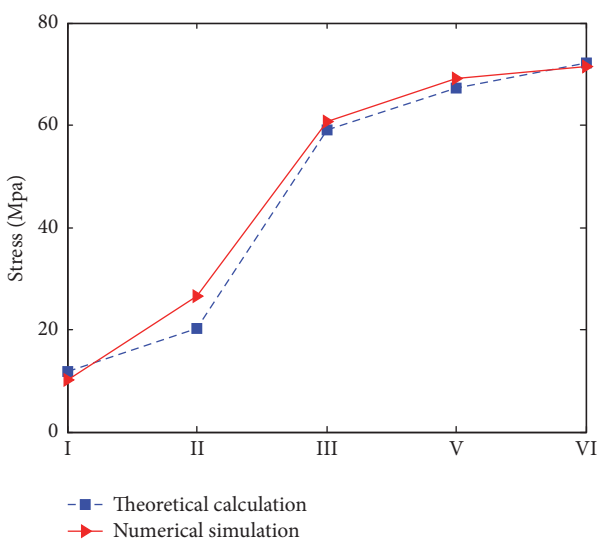

Figure 13: Comparison of theoretical and finite element solution of sectional normal stress.

theoretical method of this study basically meets the accuracy requirement of ILSD-LS design.

5. Experimental Study of ILSD-LS and LSD-LS

In order to compare the energy dissipation capacity and the stability between LSD-LS and ILSD-LS, and to further verify the accuracy of the theoretical analysis, one LSD-LS and one ILSD-LS were fabricated. The basic dimensions of both specimens are the same as those shown in Figure 9.

The low cycle reciprocating load experiments are carried out for two specimens, as shown in Figure 14. Among them, the internal structure of the lead block for lead groove of LSD-LS is shown in Figure 14(a), and the lead block is not divided. The internal structure of the lead block for lead groove of ILSD-LS is shown in Figure 14(b), and the lead block is divided into two parts by bars.

The experiments are carried out by using a 3000 kN damper test system, which can operate test on the dynamic performance of the energy dissipation dampers, such as viscous dampers, lead damper and friction damper, and so on. The test specimen is required to be 0.4 m–5 m in length and its maximum width is 1.5 m. The level of the test system allows the static tension to be 4500 kN, and the operating frequency is 0–20 Hz. In this paper, the specimen is subjected to simple harmonic loading with 0.1 Hz frequency.

The displacement-controlled method is adopted, and the loading history is shown in Figure 15. The displacement and the damping force of the damper are recorded, respectively, with a displacement meter and a force sensor.

The experimental results of the LSD-LS are shown in Figure 16. It can be seen that the yield force is inadequate under small displacement. As the loading displacement gradually increases, the yield force also increases, and the hysteresis curve appears a concave shape. It indicates that the energy consumption of the shearing block lead is insufficient and does not yield completely. As the displacement increases, local compaction state appears in the lead block near the side baffle, and the pressure between the lead block and the cover plate could increase; then the yield force increases. When the displacement reaches 60 mm, the yield force progressively deteriorates with the numbers of loading cycle increase.

The experimental results of the ILSD-LS are shown in Figure 17. It can be found out that the hysteresis curve no longer shows a concave shape, which indicates that the shearing lead block has reached the yield state under small displacement and the stress is homogeneous. During the loading process, the yield force of the ILSD-LS approximately remains about 1000 kN, which is larger than that of LSD-LS. When the displacement is 90 mm, the degradation degree of yield force is not significant with the increasing numbers of loading cycles.

According to (13), the theoretical yield force of the ILSD-LS is 946 kN. Four types of results are obtained and comparatively analyzed: the experimental result of LSD-LS at the displacement of 60 mm, the simulation results of ILSD-LS at the displacement of 90 mm, and the experimental results of ILSD-LS at the displacements of 60 mm and 90 mm, respectively, as shown in Figure 18. It can be seen that the energy dissipation capacity of LSD-LS is significantly lower than that of ILSD-LS because the relative shear lead block length of LSD-LS is longer and the damping efficiency is not high. In addition, the yield force of ILSD-LS is as large as 66.6% of the yield force of LSD-LS, and the energy dissipation of ILSD-LS is more stable. The experimental results, simulation results, and theoretical calculations of

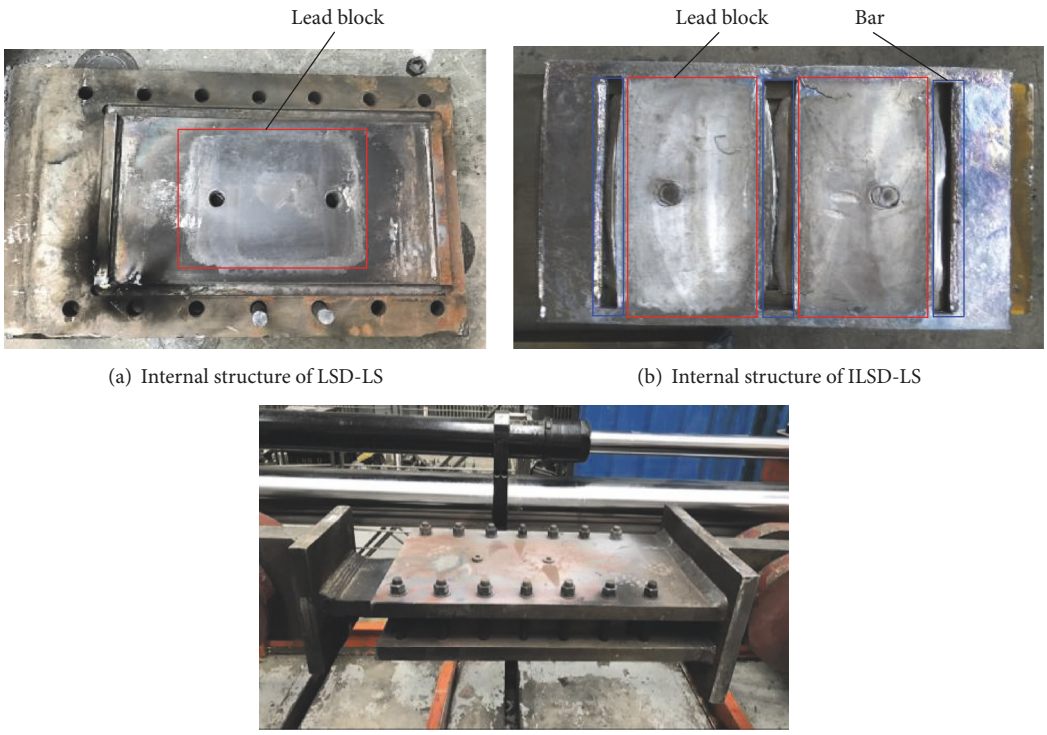

(a) Internal structure of LSD-LS

(b) Internal structure of ILSD-LS

(c) Integral specimen of damper

Figure 14: Experiment of LSD-LS.

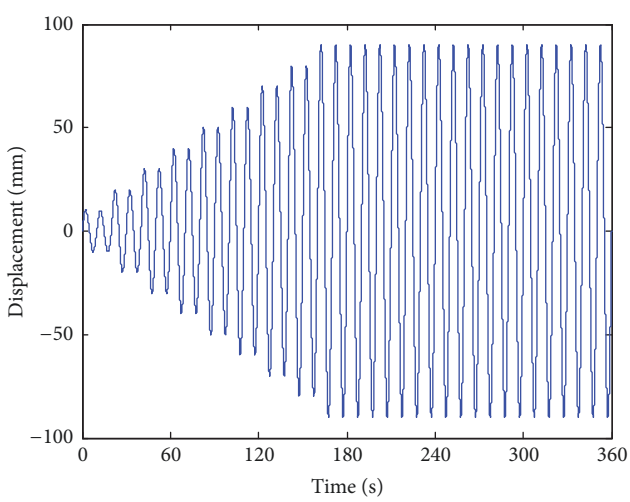

Figure 15: Loading history.

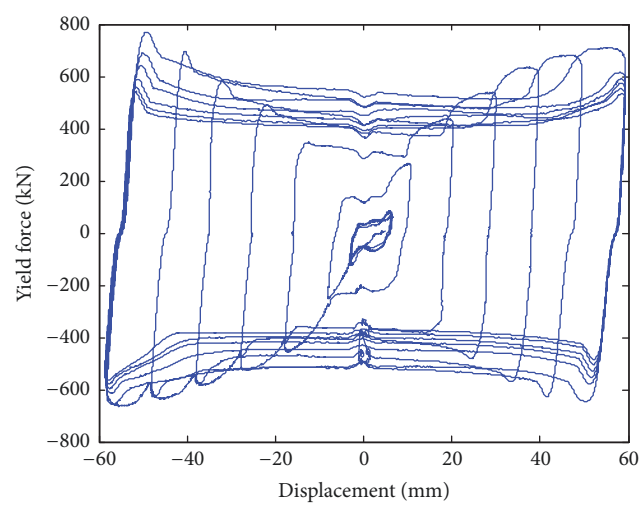

Figure 16: Experiment result of LSD-LS.

ILSD-LS are in good agreement, and the difference among the three is not more than 6%.

Taking into account the above analysis results, it can be concluded that ILSD-LS can meet the requirements of long stroke and large yield force, and its damping efficiency and stability are better than those of LSD-LS.

The above theoretical analysis, FE simulation, and experiment about ILSD-LS show that its energy dissipation performance is stable and excellent, and the following section is analyses of the control effects of a high-rise building with ILSD-LS under the action of actual ground motion.

6. Case Analysis

To verify the damping capacity of ILSD-LS on the seismic response of high-rise buildings subjected to normal ground motions and long-period ground motions, a reinforced concrete (RC) frame structure is selected as a typical case,

Table 1: Information of recorded ground motions.

Event	Station	Number	Time	Magnitude	Peak acceleration (cm/s^2)	Duration (s)
Borrego Mtn	San Onofre-SoCal Edison	T1	1968	6.6	46.30	45.20
Kern County	LA-Hollywood Stor FF	T2	1952	7.4	57.80	70.00
Imperial Valley-06	Calipatria Fire Station	T3	1979	6.5	126.22	39.63
Chi-Chi_ Taiwan-03	CHY078	T4	1999	6.2	17.15	59.00
Chi-Chi_ Taiwan	CHY054	T5	1999	7.6	93.00	77.60
Chi-Chi_ Taiwan-03	CHY107	T6	1999	6.2	45.59	90.00

and numerical analysis is carried out. The structure has 15 stories with a total height of 60 m. The RC beam section is rectangular and the dimension is 1000 mm × 700 mm, the elastic modulus of the concrete is 3.0×10^4 N/mm^2, the axial compressive strength is 14.3 N/mm^2, and the axial tensile strength is 1.43 N/mm^2. The RC column section is also rectangular, and the dimension is 900 mm × 900 mm, the elastic modulus of the concrete is 3.15×10^4 N/mm^2, the axial compressive strength is 16.7 N/mm^2, and the axial tensile strength is 1.57 N/mm^2. The RC plate thickness is 100 mm, and the elastic modulus is 3.0×10^4 N/mm^2, axial compressive strength is 14.3 N/mm^2, and axial tensile strength is 1.43 N/mm^2. The gravity loads used in the design are represented by dead- and live-loads, equal to 2.0 kN/m^2 and 2.5 kN/m^2, respectively. The site type is soft rock and the seismic precautionary intensity is 8.0, which means the structure may suffer from the earthquake whose exceeding probability of this intensity is 10% in the 50 year period, and the basic seismic acceleration value is 0.15 g. The fundamental period of the RC frame is 1.55 s. In order to enhance the structural safety, diagonal steel braces equipped with ILSD-LSs are installed on the high-rise structure. According to the dynamic characteristics of the structure, the performance parameters of the damper are as follows: the yield force is 1000 kN, the stroke is 90 mm, and the initial stiffness is 8.0×10^5 kN/m. Moreover, the properties of the ILSD-LS are assumed as the same for each story, including yield force and initial stiffness, which may be relatively low damping efficient, and the upper stories have greater stiffness than the lower stories. However, the typical RC frame structure does not have any adverse effects during earthquakes after installing ILSD-LSs, and the more optimal method for damper design and installation can consult the corresponding study by Ponzo et al. [35, 36].

In order to avoid structural eccentricity and weak stories, and considering the energy dissipation efficiency of the dampers, the ILSD-LSs are arranged along the four corners of the structure, and 8 dampers are installed for each story; thus, the total number of ILSD-LSs is 120. The elastic-plastic structural model is established in SAP2000, as shown in Figure 19, in which the beam and column are modeled by beam-column element, and the ILSD-LS is simulated by

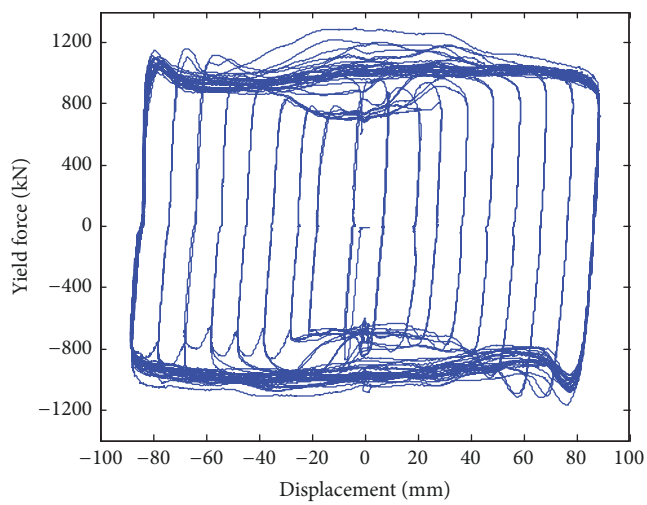

Figure 17: Experiment result of ILSD-LS.

LINK elements, and the LINK element setting property is plastic (Wen) model. On this basis, the nonlinear dynamic time history analysis considering single-dimensional ground motions is carried out.

In this study, in order to investigate the influence of long-period ground motion on the response of dampers and structure, and the technical requirements of ILSD-LS, 6 natural ground motion records are selected, and the specific information is shown in Table 1. In accordance with the code for seismic design of buildings in China, the peak acceleration of all the waves is adjusted to 400 cm/s^2, and the corresponding acceleration response spectra are shown in Figure 20. The six waves are input along the long-axis direction; then the structural elastic-plastic time history analysis is carried out.

By analyzing the structural dynamic responses, it indicates that the interstory drifts of the structure under long-period ground motions are obviously larger than that of the normal ground motions. When the uncontrolled structure is subjected to long-period ground motions, the maximum interstory drift can reach 72.6 mm. Since the biggest interstory drift usually occurs on the fourth story, the corresponding results that are interstory drift and acceleration of this

Table 2: Peak damping ratio of different ground motions (%).

Wave number	T1	T2	T3	T4	T5	T6
Interstory drift angle	36.27	36.21	34.14	45.35	42.92	41.08
Peak acceleration	0.32	−4.13	−8.5	−1.05	−4.66	0.68
Base shear force	0.27	1.01	23.71	6.18	26.78	6.46

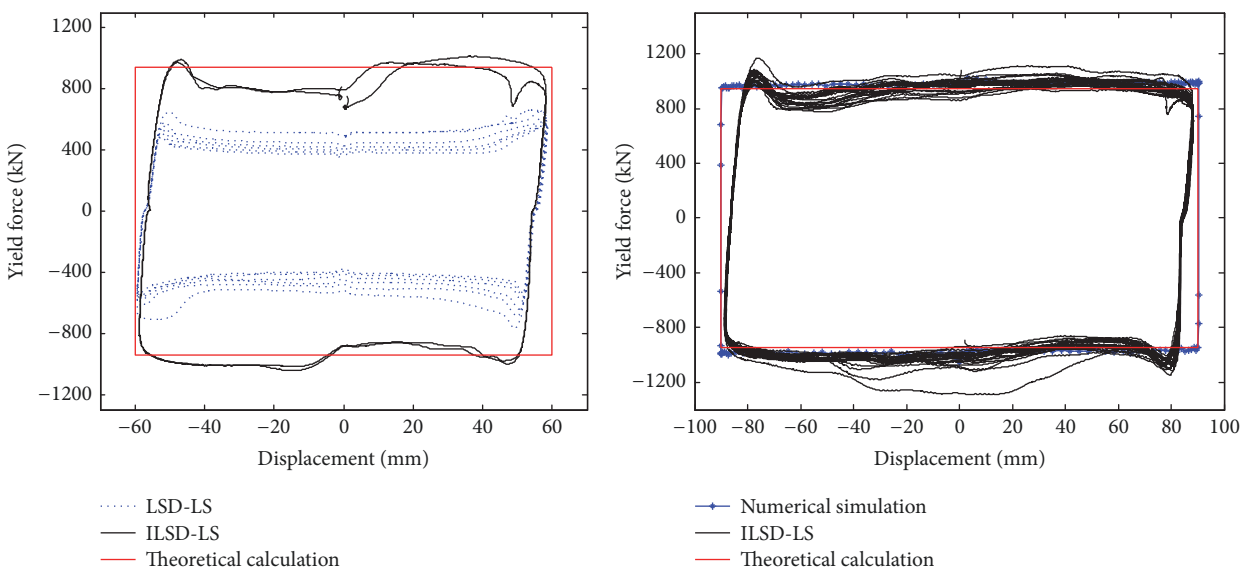

(a) Displacement 60 mm (b) Displacement 90 mm

Figure 18: Comparison of hysteretic curves with different displacement amplitude.

story before and after control is chosen and compared, and the responses under wave T1 and wave T4 are shown in Figures 21 and 22, respectively. The results show that ILSD-LS can effectively reduce the story drift. In contrast, the stroke of ordinary lead shear damper usually cannot be reached more than 40 mm, though the stroke of LSD-LS may meet the basic requirements; however, its energy dissipation capacity is insufficient. Hence, the superior damping effect as ILSD-LS cannot be obtained if the ordinary dampers or LSD-LSs are adopted.

To further discuss the effect of ground motion on the seismic response of the structure with ILSD-LS, the damping ratio of peak interstory drift angle is calculated, as listed in Table 2. The typical interstory drift angle before and after control is shown in Figure 23. The damping effect of the dampers is obvious so the damping capacity of ILSD-LS for the overall response of the high-rise structure is further verified.

In addition, the damping effect of peak acceleration is also compared and analyzed, and the results are shown in Table 2. The typical contrast results are shown in Figure 24. The partial peak acceleration value increases after installing dampers because ILSD-LS provides additional stiffness to the structure. As a result, the structural periods slightly decrease and the seismic reaction increases. In view of amplification of acceleration being insignificant and the damping effect of displacement being obvious, the corresponding adverse effects can be accepted.

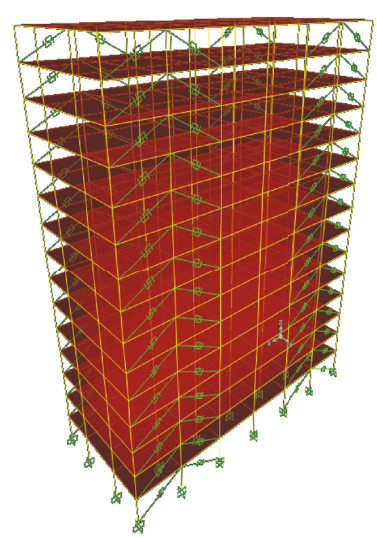

Figure 19: Finite element analysis model.

Furthermore, the damping ratio of different stories is diverse. The damping effect of the top story is the worst because the interstory drift is smaller and the ILSD-LS does

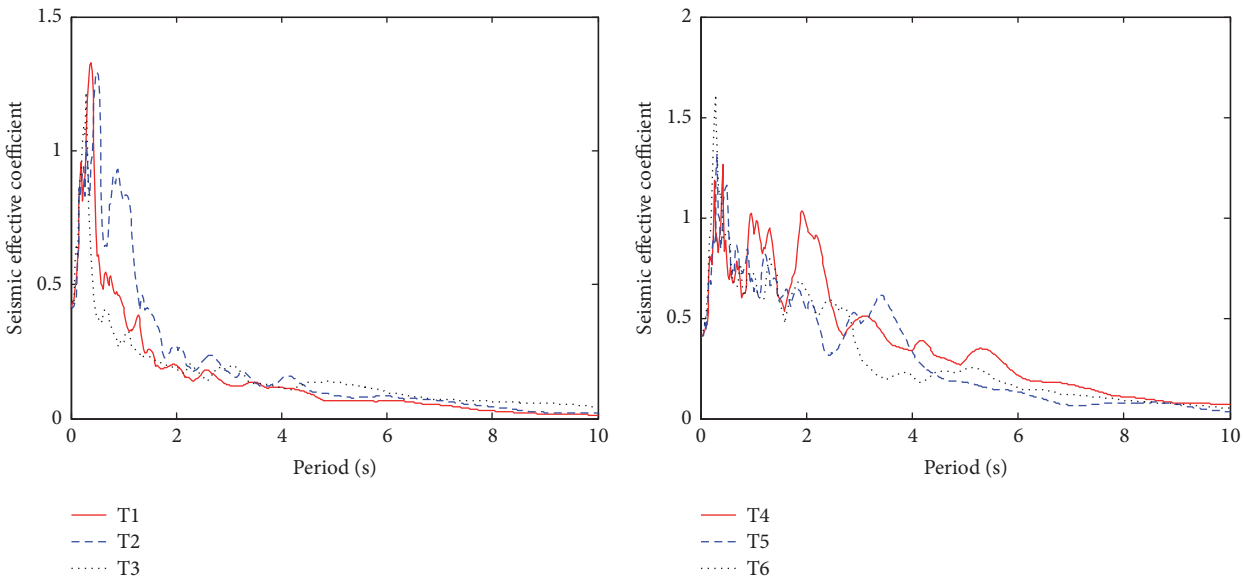

(a) Spectra of normal earthquakes (b) Spectra of long-period earthquakes

Figure 20: Acceleration response spectra.

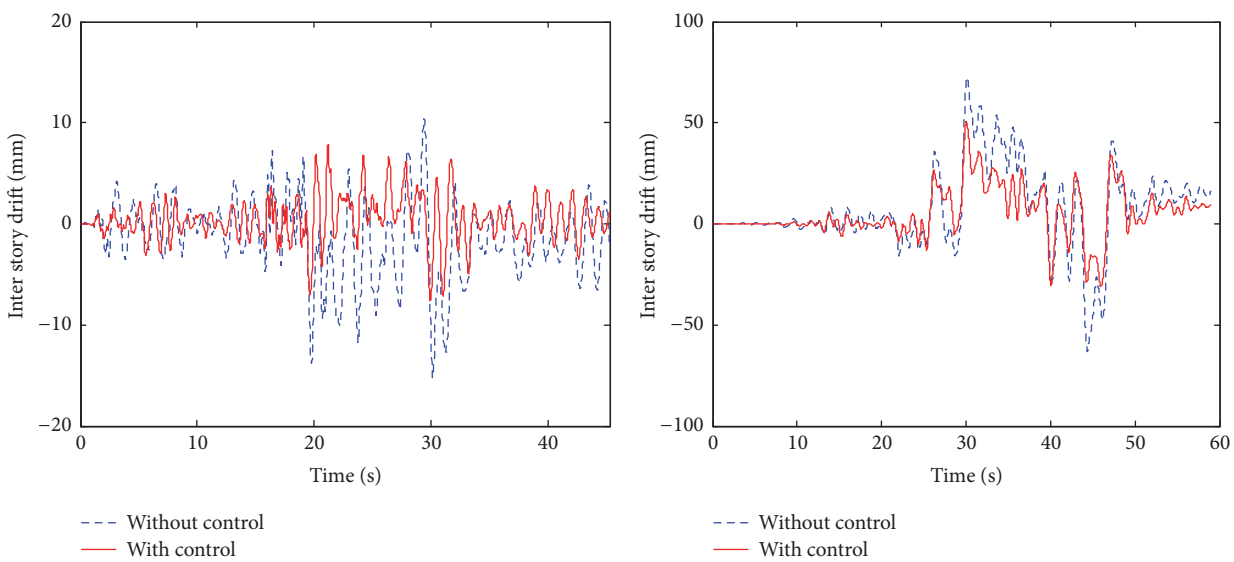

(a) Results of Wave T1 (b) Results of Wave T4

Figure 21: Interstory drift time history of different earthquakes.

not reach yield stage, so the kinetic energy is not necessarily dissipated and the damper provides only lateral stiffness.

In addition, the base shear force that is the shear of the bottom of the first story columns of the structure with or without control is compared, as shown in Figure 25. The damping effect of base shear force is also compared and analyzed, and the results are shown in Table 2. The results show that the force of the main body of the structure is obviously decreased, and the structural safety is improved. The hysteretic curves of ILSD-LS under the action of ground motion are shown in Figure 26; the results indicate that the damping capacity of the damper is excellent, and the long stroke adequately meets the requirement for the long-period ground motions.

In order to further represent the ductility demand for the RC members to better enlighten the effectiveness of the ILSD-LSs, the hysteretic curves of the typical column at the bottom are compared without and with control under Wave T3, as shown in Figure 27, where the displacement refers to the displacement of the top of the column relative to the bottom, and the shear force refers to the shear force at the top of the column. The columns located between two diagonal braces with ILSD-LSs at first, fourth, and seventh stories are selected. The hysteretic curves of column of the first story

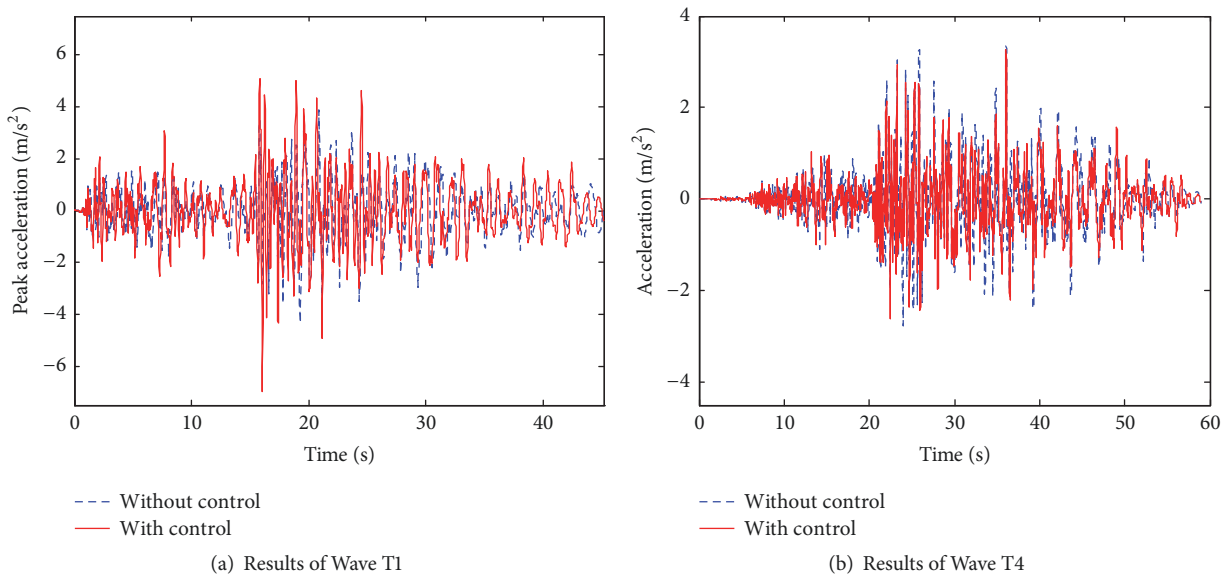

(a) Results of Wave T1

(b) Results of Wave T4

Figure 22: Acceleration time history of different earthquakes.

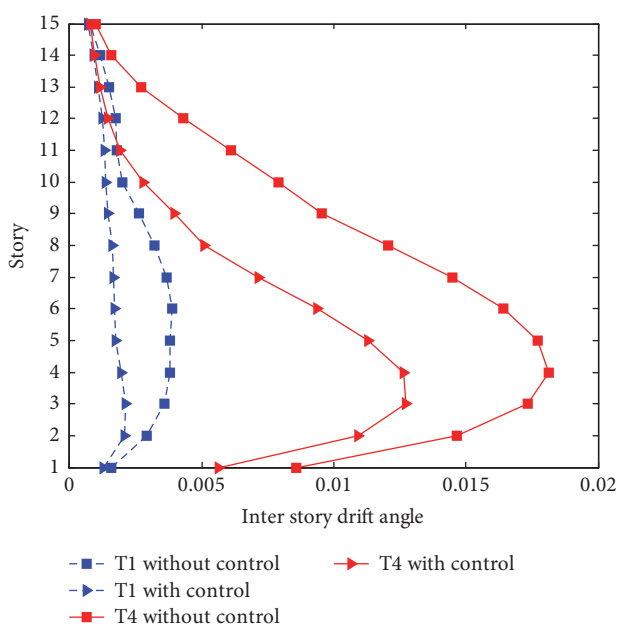

Figure 23: Interstory drift angle for different ground motions.

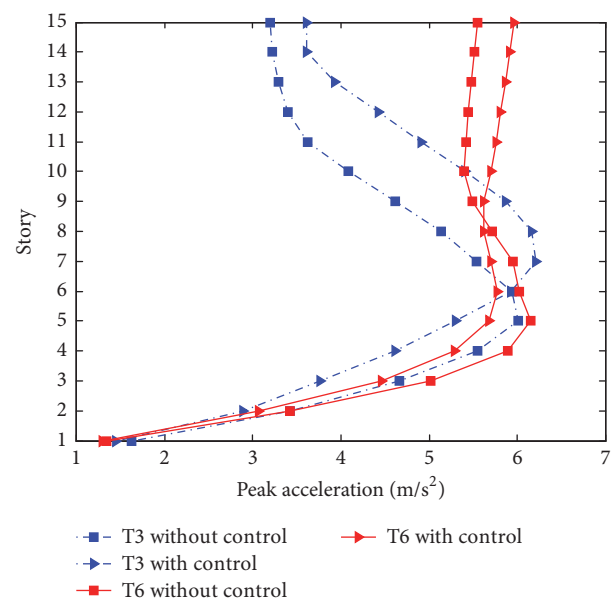

Figure 24: Peak acceleration before and after control.

are shown in Figure 27(a), and the maximum displacement without or with control is 6.24 mm or 5.11 mm, respectively. The hysteretic curves of column of the fourth story are shown in Figure 27(b); the maximum displacement without or with control is 15.22 mm or 7.66 mm, respectively. The hysteretic curves of column of the seventh story are shown in Figure 27(c), and the maximum displacement without or with control is 14.7 mm or 6.71 mm, respectively. The results show that the ductility demand and seismic performance of the original RC frame structural members are also improved.

The above results prove that ILSD-LS is effective in decreasing the seismic response of the high-rise buildings. Although the structural responses under long-period ground motions are significantly greater than those of normal ground motions, the damping effect of the structure under the long-period ground motions is better because ILSD-LS has the advantages of long stroke, adequate energy dissipation, and good stability.

7. Conclusions

In this study, in order to reduce large deformation of the high-rise building structure which is subjected to far-field earthquake with long-period components, an improved lead shear damper of large stroke (ILSD-LS) is presented, and

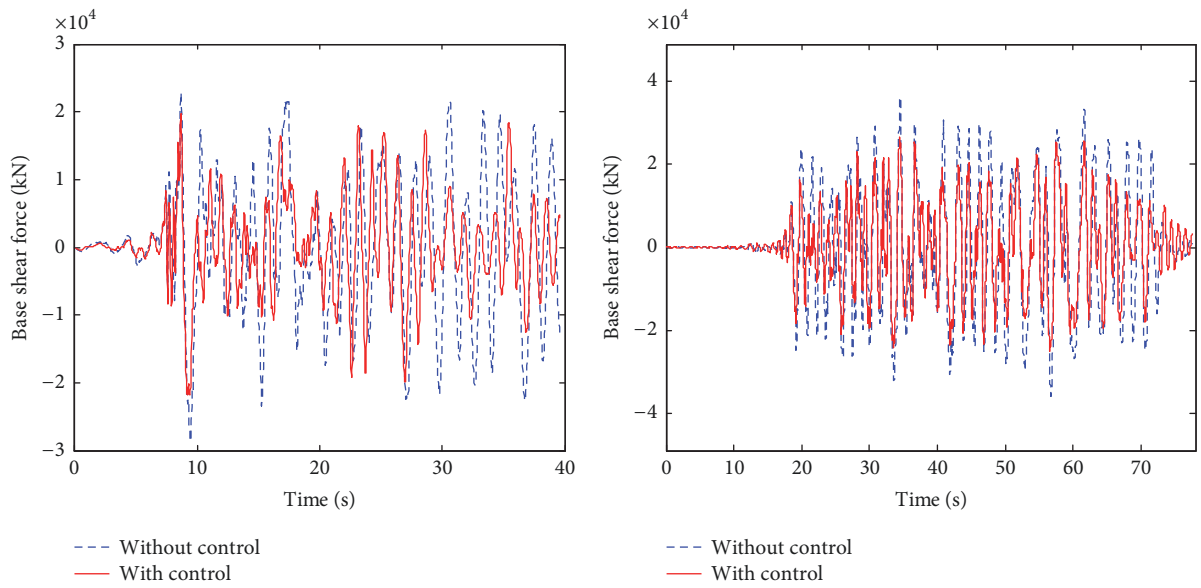

(a) Results of Wave T3

(b) Results of Wave T5

Figure 25: Base shear force time history of different ground motions.

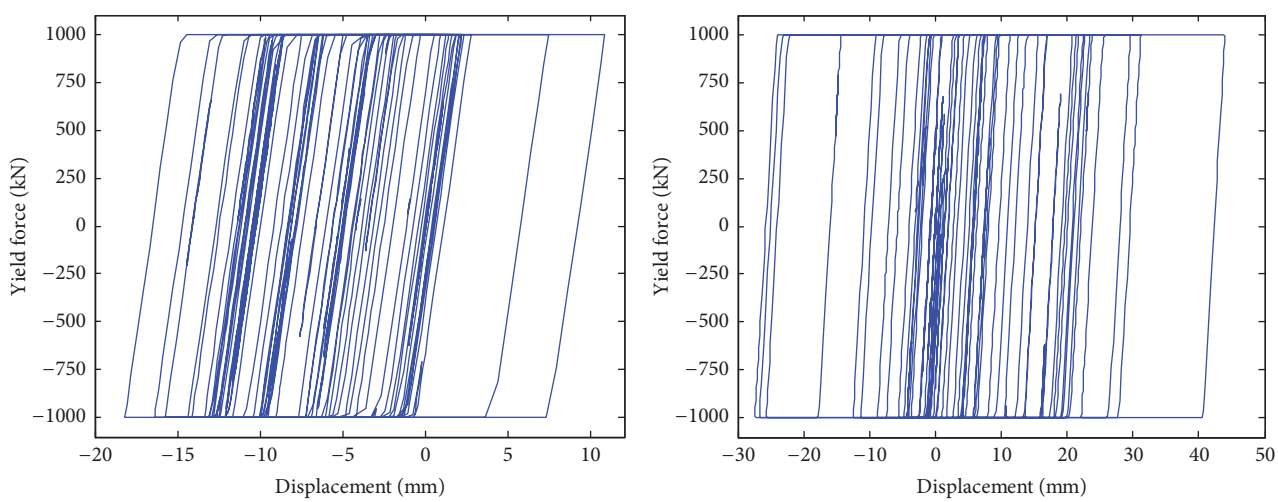

(a) Results of Wave T2

(b) Results of Wave T4

Figure 26: Hysteretic curves of ILSD-LS of different ground motions.

the mechanical structure of the damper is introduced. The theoretical analytic solutions, numerical simulation, and experimental research on the mechanical model of the ILSD-LS are carried out. Finally, the damper is applied to a high-rise building subjected to ground motions and the corresponding dynamic time history analysis is carried out. The results show that the energy dissipation capacity of ILSD-LS is stable and fine. The ILSD-LSs can effectively control the deformation and reduce the damage of the high-rise building structure especially for long-period earthquakes, and their beneficial effects can be improved proportioning them by some optimal design procedure according to a corresponding study [35, 36]. The main conclusions are obtained as follows:

(1) Based on the ideal rigid-plastic constitutive law of lead, considering the extrusion effect of the bars on the sliding plate, a mechanical model of the ILSD-LS is established, and the damping force formula is proposed and its correctness is verified.

(2) With contrast experiments on the LSD-LS and the ILSD-LS, it is evident that the energy dissipation capacity and the stability of the ILSD-LS are better, which could meet the requirements for stroke and yield force.

(3) Taking an actual reinforced concrete frame as an analysis example, the nonlinear time analysis is carried out, and the effects of normal and long-period ground motions are considered. The numerical results indicate that dynamic

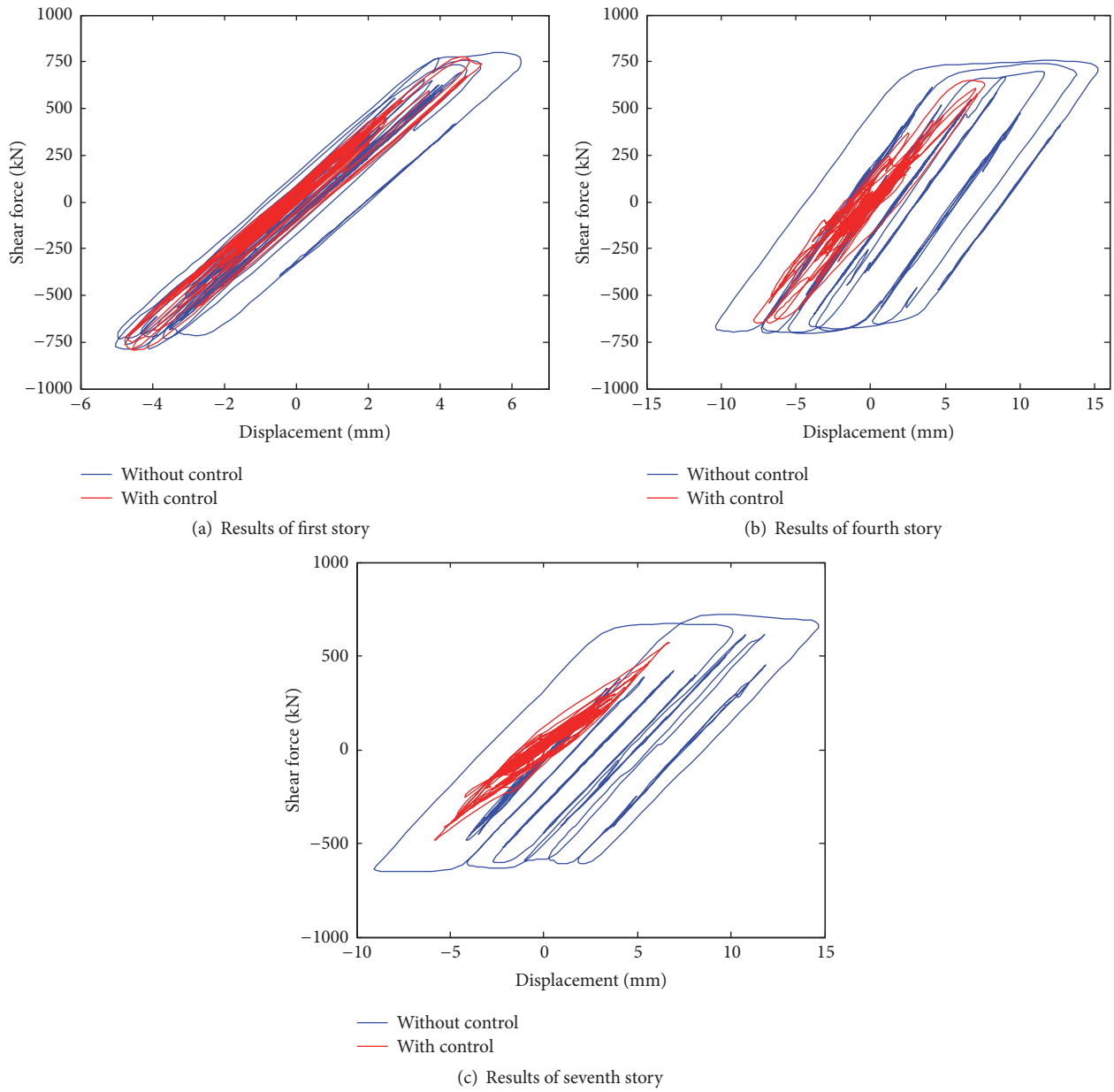

Figure 27: The hysteretic curves of the typical column.

responses of the high-rise structure with ILSD-LS significantly decrease, even when the structure is subjected to long-period ground motion.

Although the damping effect of ILSD-LS has been verified, the dampers are installed on all stories for structural nonlinear analysis in this study, so the cost-benefit ratio is higher. For the complex structures with uneven story stiffness or eccentric structure, how to select the effective control index to optimize the damping parameters and installation location of ILSD-LS still needs to be studied.

Conflicts of Interest

The authors declare that there are no conflicts of interest regarding the publication of this paper.

Acknowledgments

This work is partially supported by Natural Science Foundation of China under Grant nos. 51378039, 51421005, 51478024, and 91315301-03.

References

[1] T. Ariga, Y. Kanno, and I. Takewaki, "Resonant behaviour of base-isolated high-rise buildings under long-period ground motions," *The Structural Design of Tall and Special Buildings*, vol. 15, no. 3, pp. 325–338, 2006.

[2] D. Kim and J. Kim, "Experimental Study on the Structural Performance of Hybrid Friction Damper," *Journal of the Korean Association for Spatial Structures*, vol. 15, no. 3, pp. 103–110, 2015.

[3] I. H. Mualla and B. Belev, "Performance of steel frames with a new friction damper device under earthquake excitation," *Engineering Structures*, vol. 24, no. 3, pp. 365–371, 2002.

[4] K.-W. Min, J.-Y. Seong, and J. Kim, "Simple design procedure of a friction damper for reducing seismic responses of a single-story structure," *Engineering Structures*, vol. 32, no. 11, pp. 3539–3547, 2010.

[5] R.-H. Zhang, T. T. Soong, and P. Mahmoodi, "Seismic response of steel frame structures with added viscoelastic dampers," *Earthquake Engineering & Structural Dynamics*, vol. 18, no. 3, pp. 389–396, 1989.

[6] Z. Pawlak and R. Lewandowski, "The continuation method for the eigenvalue problem of structures with viscoelastic dampers," *Computers & Structures*, vol. 125, pp. 53–61, 2013.

[7] J.-D. Kang and H. Tagawa, "Seismic response of steel structures with seesaw systems using viscoelastic dampers," *Earthquake Engineering & Structural Dynamics*, vol. 42, no. 5, pp. 779–794, 2013.

[8] A. D. E. Pan and N. Yeung, "Wind tunnel experiments of a building model incorporating viscous-damping walls," *Wind and Structures, An International Journal*, vol. 4, no. 3, pp. 261–276, 2001.

[9] C. A. Martínez, O. Curadelli, and M. E. Compagnoni, "Optimal design of passive viscous damping systems for buildings under seismic excitation," *Journal of Constructional Steel Research*, vol. 90, pp. 253–264, 2013.

[10] E. Tubaldi, L. Ragni, and A. Dall'Asta, "Probabilistic seismic response assessment of linear systems equipped with nonlinear viscous dampers," *Earthquake Engineering & Structural Dynamics*, vol. 44, no. 1, pp. 101–120, 2015.

[11] C. Zhang, Z. Zhang, and J. Shi, "Development of high deformation capacity low yield strength steel shear panel damper," *Journal of Constructional Steel Research*, vol. 75, pp. 116–130, 2012.

[12] S. Maleki and S. Bagheri, "Pipe damper, Part I: Experimental and analytical study," *Journal of Constructional Steel Research*, vol. 66, no. 8-9, pp. 1088–1095, 2010.

[13] R. W. K. Chan and F. Albermani, "Experimental study of steel slit damper for passive energy dissipation," *Engineering Structures*, vol. 30, no. 4, pp. 1058–1066, 2008.

[14] K. Ghabraie, R. Chan, X. Huang, and Y. M. Xie, "Shape optimization of metallic yielding devices for passive mitigation of seismic energy," *Engineering Structures*, vol. 32, no. 8, pp. 2258–2267, 2010.

[15] E. Matta, "Effectiveness of tuned mass dampers against ground motion pulses," *Journal of Structural Engineering (United States)*, vol. 139, no. 2, pp. 188–198, 2013.

[16] K. Tarbali and F. Nateghi-A, "Effect of structural uncertainty on seismic response of steel moment-resisting frames equipped with tuned mass dampers," *International Journal of Steel Structures*, vol. 14, no. 2, pp. 231–241, 2014.

[17] A. Lucchini, R. Greco, G. C. Marano, and G. Monti, "Robust design of tuned mass damper systems for seismic protection of multistory buildings," *Journal of Structural Engineering (United States)*, vol. 140, no. 8, Article ID A4014009, 2014.

[18] Y. Chen, D. M. McFarland, Z. Wang, B. F. Spencer Jr., and L. A. Bergman, "Analysis of tall buildings with damped outriggers," *Journal of Structural Engineering*, vol. 136, no. 11, pp. 1435–1443, 2010.

[19] Y. M. Parulekar, G. R. Reddy, K. K. Vaze, and H. S. Kushwaha, "Lead extrusion dampers for reducing seismic response of coolant channel assembly," *Nuclear Engineering and Design*, vol. 227, no. 2, pp. 175–183, 2004.

[20] C. S. Tsai, W. S. Lai, C. W. Chang, and M. C. Li, "Testing and analysis of a new lead-extrusion damper," in *Proceedings of the Seismic Engineering -2002- (2002 ASME Prssure Vessels and Piping Conference)*, pp. 215–220, Canada, August 2002.

[21] D. Zhou, W. Yan, Y. Chen, and C. Liu, "Seismic analysis of a low tower cable-stayed bridge and application of lead shear damper," *Applied Mechanics and Materials*, vol. 90-93, pp. 1715–1719, 2011.

[22] R. O. Curadelli and J. D. Riera, "Design and testing of a lead damper for seismic applications," *Proceedings of the Institution of Mechanical Engineers, Part C: Journal of Mechanical Engineering Science*, vol. 221, no. 2, pp. 159–165, 2007.

[23] G. W. Rodgers, J. G. Chase, J. B. Mander, N. C. Leach, and C. S. Denmead, "Experimental development, tradeoff analysis and design implementation of high force-to-volume damping technology," *Bulletin of the New Zealand Society for Earthquake Engineering*, vol. 40, no. 2, pp. 35–48, 2007.

[24] W. H. Robinson and L. R. Greenbank, "An extrusion energy absorber suitable for the protection of structures during an earthquake," *Earthquake Engineering & Structural Dynamics*, vol. 4, no. 3, pp. 251–259, 1976.

[25] M. D. Monti and W. H. Robinson, "A lead shear damper suitable for reducing the motion induced by wind and earthquake," in *Proceedings of the 11 WCEE*, vol. 271, p. 271, Mexico, Acapulco, Mexico.

[26] Y. Q. Ni, H. J. Liu, and J. M. Ko, "Experimental investigation on seismic response control of adjacent buildings using semi-active MR dampers," in *Proceedings of the Smart Structures and Materials 2002: Smart Systems for Bridges, Structures, and Highways*, pp. 334–344, USA, March 2002.

[27] S. Behrens, A. J. Fleming, and S. O. Reza Moheimani, "Electromagnetic shunt damping," in *Proceedings of the 2003 IEEE/ASME International Conference on Advanced Intelligent Mechatronics, AIM 2003*, pp. 1145–1150, Japan, July 2003.

[28] X. Zhou and L. Peng, "A new type of damper with friction-variable characteristics," *Earthquake Engineering and Engineering Vibration*, vol. 8, no. 4, pp. 507–520, 2010.

[29] K. Minagawa, S. Fujita, T. Kawamura, and G. Tanaka, "Seismic response analysis of industrial building with viscous-friction hybrid damper," in *Proceedings of the ASME 2013 Pressure Vessels and Piping Conference, PVP 2013*, France, July 2013.

[30] A. M. Sharabash and B. O. Andrawes, "Application of shape memory alloy dampers in the seismic control of cable-stayed bridges," *Engineering Structures*, vol. 31, no. 2, pp. 607–616, 2009.

[31] X. Shen, X. Wang, Q. Ye, and A. Ye, "Seismic performance of Transverse Steel Damper seismic system for long span bridges," *Engineering Structures*, vol. 141, pp. 14–28, 2017.

[32] D. Zhou, *Study on Seismic Performance of Long-Span Girder Bridges Considering Soil and Structure Interaction*, Beijing University of Technology, 2012.

[33] J. L. Wen, H. Ding, and F. R. Cao, *Extrusion and Drawing Technology for Non-Ferrous Metals*, chemical industry press, Beijing, China, 2007.

[34] L. Y. Peng, W. M. Yan, and H. X. He., "Finite element analysis and testing of plate type shear lead damper," *Journal of Vibration and Shock*, vol. 29, no. 1, pp. 183–189, 2010.

[35] F. C. Ponzo, A. Di Cesare, D. Nigro et al., "Jet-pacs project: dynamic experimental tests and numerical results obtained for a steel frame equipped with hysteretic damped chevron braces," *Journal of Earthquake Engineering*, vol. 16, no. 5, pp. 662–685, 2012.

[36] A. Di Cesare and F. C. Ponzo, "Seismic retrofit of reinforced concrete frame buildings with hysteretic bracing systems: design procedure and behaviour factor," *Shock and Vibration*, vol. 2017, Article ID 2639361, 20 pages, 2017.